Influence of Hot-Melt Extrusion and Compression Molding on Polymer Structure Organization, Investigated by Differential Scanning Calorimetry

A. G. SARRAF,[1] H. TISSOT,[2] P. TISSOT,[2] D. ALFONSO,[1] R. GURNY,[1] E. DOELKER[1]

[1] University of Geneva, School of Pharmacy, CH-1211 Geneva 4, Switzerland

[2] University of Geneva, Department of Inorganic, Analytical and Applied Chemistry, CH-1211 Geneva 4, Switzerland

Received 7 January 2000; accepted 20 September 2000

ABSTRACT: A blend of a pullulan polymer and 1,2,6-hexanetriol as a plasticizer were used to study the effect of melt processing techniques on the physical properties of the resulting materials. The main advantage of pullulan is its linear polysaccharide chain model structure. Hot-melt extrusion and compression molding were performed under the same temperature and pressure conditions. The materials obtained were analysed by differential scanning calorimetry. For the first time, the comparative effect of the two processing techniques, i.e., extrusion and compression molding, on the polymer arrangement is reported. Endothermic events resulted from the melt extrusion process were shown to be related to different structures of oriented populations of macromolecules and to microphase separation. Orientation was enhanced by cooling the extrudate at the die exit, with a corresponding increased enthalpy from 34.7 to 51.4 J/g. In contrast, when using compression molding, the endotherm was less marked (11.9 J/g), suggesting less orientation, but the shape of the thermogram was quite similar to that of the extrudate. In both cases, we observed a loss of orientation when the molded materials were milled. A semiquantitative kinetic study of the disorientation process of the extrudate upon isothermic tempering suggests that a disorientation phenomenon occurs at the same time as a swelling process due to the presence of microphase separation. The extrudate was shown to be stable at 25°C. © 2001 John Wiley & Sons, Inc. J Appl Polym Sci 81: 3124–3132, 2001

Key words: hot-melt extrusion; compression molding; macromolecular orientation; phase separation; polymer; pullulan; differential scanning calorimetry; kinetics of disorientation

INTRODUCTION

The properties of polymeric materials can be decisively influenced by the manufacturing and processing method.[1,2] The sensitivity of polymers to processing conditions is, in general, greater than that of other materials. Thus, fabrication-controlled microstructural differences can provide order of magnitude variations in physical and chemical properties of a given polymer. In particular, attributes such as orientation, molecular weight, and crystallinity are often affected by the processing techniques used to convert a thermoplastic material.[3–5]

During extrusion molding, when polymers are heated and stretched, orientation can be

Correspondence to: E. Doelker (eric.doelker@pharm.unige.ch).

Journal of Applied Polymer Science, Vol. 81, 3124–3132 (2001)

imparted to the material as a result of polymer flow. This polymer flow can also be generated similarly by other thermoforming processes, such as blow molding, calendering, compression molding, and injection molding. Differences arise principally from the different ranges of mechanical stress (or strain) applied to a polymeric material.[6]

Among the many advantages of hot-melt techniques compared to the traditional compression methods used in pharmaceutical technology, we can cite the minimal porosity of the manufactured dosage forms.[7] This characteristic is often sought for controlled released dosage forms. It is also well known that drug release kinetics is largely influenced by the microstructural properties.[8] Therefore, characterization of microstructures obtained from melting processes is of a great importance for understanding the drug release behavior.

To our knowledge this is the first time that comparative effect of the two processing techniques i.e., extrusion and compression molding, on the polymer arrangement is investigated.

In this paper, pullulan (PU), the major constituent of the melted material, was chosen as a linear chain model. It provides initial basic information for understanding more complex polysaccharide structures (branched, charged, etc.). PU is an amorphous, water-soluble, nonionic polysaccharide that has found wide application in microbiology and food.[9] It is produced from starch by cultivating a black yeast, *Aureobasidium pullulans*. This polymer consists of maltotriose units or amylose fragments (α-D-glucopyranosyl-(1 $\rightarrow$ 4)-α-D-glucopyranosyl-(1 $\rightarrow$ 4)-α-D-glucose) linked by α-(1 $\rightarrow$ 6) bonds.[10]

Pullulan cannot be extruded without the addition of a plasticizer. A preliminary study has shown that 1,2,6-hexantriol, which has already been used as a plasticizer with starch,[11] is the most convenient.

The same blends were processed by extrusion and compression molding under the same temperature and pressure, unless otherwise stated. Differential scanning calorimetry was used to characterize and compare extrudate and molded tablet structures. The relative influences of molding techniques on the polymer arrangement are highlighted. Furthermore, the effect of isothermal conditioning on the melted materials was studied at different temperatures.

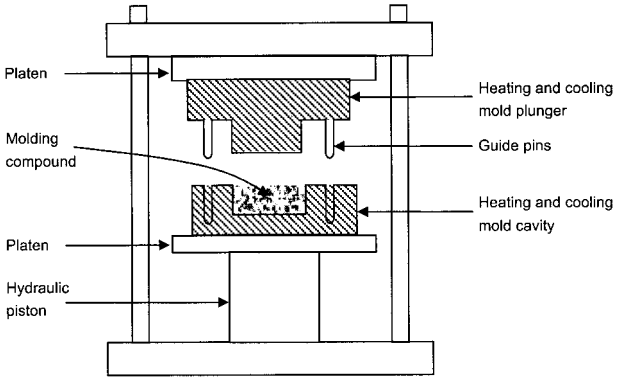

Figure 1 Compression molder.

MATERIALS AND METHODS

Materials

Pullulan (M_w: 70000) present as the major constituent of the melted material and 1,2,6-hexanetriol (M_w: 134) as a plasticizer were supplied by Fluka Chemie AG, Switzerland. To remove water, pullulan was placed in an oven at 50°C until constant weight was observed.

Methods

Powder Blend

Pullulan was added with 1,2,6-hexantriol (90/10 w/w) in a mortar and the mixture was then blended for one hour in a Turbula T2A (Basel, Switzerland).

Melt Extrusion

The blend powder was sintered in the laboratory ram extruder[7] to minimize trapped air bubbles in the extrudate. After 5 min of preheating at 160°C, the blend was extruded at the same temperature under appropriate pressure. The inside barrel diameter was 10 mm. The capillary had a 2-mm diameter, with a length/diameter ratio of 9 (L/D = 9). The entrance of the capillary was tapered with a half-cone angle of 45°.

Compression Molding

The apparatus used was a specially designed compression molder equipped with heating and cooling stainless steel molds fixed on two platens (Fig. 1). The 10-mm mold cavity diameter was made in a stainless steel sheet of 0.5 cm thickness attached to the lower platen.

Molded tablets were prepared by filling the cavity with 130 mg powder blend. The upper and lower platens of the assembly were pressed together under 160 MPa by a Specac hydraulic press (Sidcup, Kent, UK). The temperature was set at 160°C. In order to cool the samples, the heating element was unplugged, and cold water circulated through the platens for at least 3 min, unless otherwise stated. Then, the pressure was released, the plate assembly removed and molded tablets (thickness = 2 mm) were ejected from the mold using an extractor at a mild pressure.

Differential Scanning Calorimetry (DSC)

A Seiko DSC 220C (Seiko Instruments, Inc., Japan) calibrated with indium was used. A sample mass, approximately 10 mg, was weighed into aluminium open pans. Processed materials (by extrusion or compression molding) were analyzed by DSC before and after freeze-milling using a Spex 6700 freeze mill (Industries, Inc., Edison, NJ, USA). In this latter case, the particle size and the uniformity of the milled fractions were determined with a long bench Malvern Mastersizer S (Malvern, UK).

The thermogram was recorded against a reference open pan placed in the reference side. A heating rate of 4°C/min with a nitrogen purge was employed throughout the characterization study, whereas a heating rate of 12°C/min was preferred for the kinetic study. At least two replicates were made for each DSC thermogram.

Thermogravimetric Analysis (TGA)

Studies were conducted using a thermogravimetric analyzer Seiko TG/DTA 220 (Seiko Instruments, Inc., Japan) calibrated using nickel. Each sample was placed in an aluminium open pan, and heated at 4°C/min under nitrogen purge.

RESULTS AND DISCUSSION

Water Content in Pullulan

Thermal behavior of undried PU during the first and second run is shown in Figure 2. The large endotherm peak observed from 20 to 130°C, which disappears during the second heating [Fig. 2(b)] most probably occurs because water is present in the sample. To verify this assumption, we calculated the number of moles of water per mole of polymer from the enthalpy of desorption

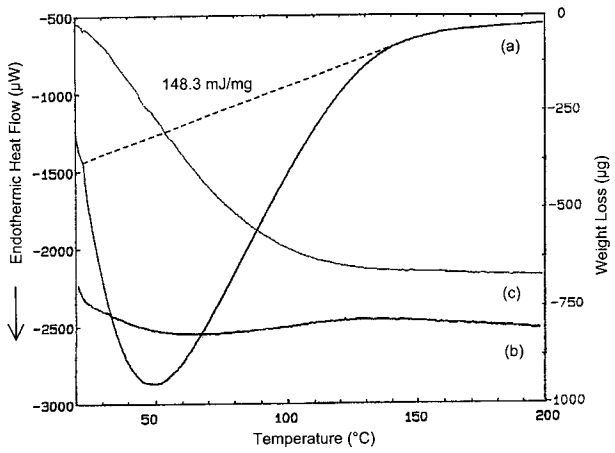

Figure 2 Thermograms of water desorption from PU. (a) DSC first run, (b) DSC second run, and (c) thermogravimetry.

ΔH_{desorp} obtained from the peak of the first heating run [Fig. 2(a)]:

$$n = \frac{M_w(\text{PU})\Delta H_{\text{desorp}}}{M_w(\text{H}_2\text{O})(\Delta H_{\text{vap}} - \Delta H_{\text{desorp}})} \quad (1)$$

where ΔH_{vap} is the specific enthalpy of vaporisation of water (2261 J/g)[12] and M_w is the molecular weight. This calculation is based on the hypothesis[13] that the enthalpy of desorption ΔH_{desorp} of n moles of water molecules present in one mole of polymer is the same as that of n moles of water molecules in liquid water ($n\Delta_{\text{vap}}H$), i.e., $\Delta H_{\text{desorp}} \cong n\Delta H_{\text{vap}}$. The n value of 271 obtained by DSC is in a good agreement with the value of 263 obtained by TGA [Fig. 2(c)]. Consequently, the endotherm from 20 to 130°C is attributed to the loss of water during the heating.

The Pullulan–Plasticizer Blend

The physical mixture exhibits a thermogram (Fig. 3) with the same shape as that in Figure 2, between 20 and 130°C, but that has a different shape above 130°C. An endothermic event is observed beyond 130°C with a maximum at 170°C, which goes up toward the baseline at 180°C [Fig. 3(a)]. This enthalpy change (9.4 J/g) observed between 130 and 180°C disappears during the second run [Fig. 3(b)].

When solvent molecules are brought into contact with amorphous polymers (e.g., pullulan), they enter their disorganized portions. They provoke a lowering of the chemical potential of the polymer segments, in particular, because of the

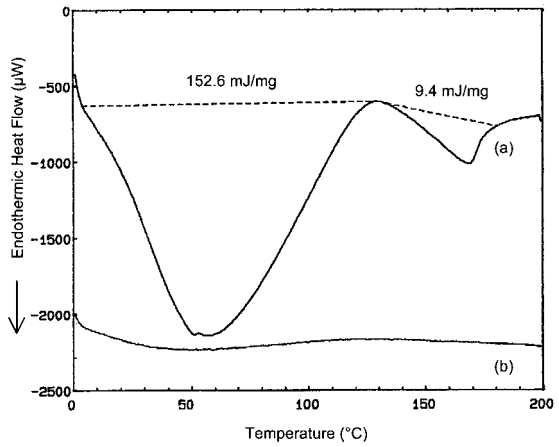

Figure 3 Thermogram of physical mixture "PU–plasticizer." (a) DSC first run, and (b) DSC second run.

entropy of exchange. The straightforward explanation of such phenomenon is the existence of segments with different chemical potentials[14,15] in pure amorphous macromolecules. Only the segments with the highest potentials can interact with the solvent molecules. Consequently, the polymer swells and the swelling is even greater than for semicrystalline polymers where large crystalline parts remain not solvated. The rate of swelling, because of high polymer viscosity, will depend to a great deal on the method of preparation, the contact time with solvent, and temperature to which the mixture is subjected. Hence, at a temperature higher than 130°C we observed by DSC the relative endotherm (9.4 J/g) of a spontaneous swelling reaction between the polymer and plasticizer.

The presence of segments with different chemical potentials in amorphous macromolecules suggests that the amorphous solid polymers in the blend are to be treated like semicrystalline polymers involved in liquid–solid phenomenon.

The Gibbs free energy of dissolution ΔG_{diss} given by[16]:

$$\Delta G_{\text{diss}} = G - G^0 = \Delta H_{\text{diss}} - T\Delta S_{\text{diss}} \qquad (2)$$

will characterize the blend formed. G^0 and G are the Gibbs free energies of the initial and final state; G^0 is obtained from the separate pure compounds (solvent and polymer). Dissolution is due to the rupture of polymer–polymer and solvent–solvent interaction forces, which are partially substituted by polymer–solvent interaction forces. Despite the fact that the enthalpy term is not favorable, Fig. 3(a) (endothermic process), the dissolution or swelling occurs because of the entropy term. In such a case, appearance of new phases is not expected as long as:

$$\text{lowest } (\mu_m)_\alpha \leq \text{lowest } (\mu_m)_\beta \qquad (3)$$

where the lowest chemical potentials $(\mu_m)_\alpha$ and $(\mu_m)_\beta$ are respectively encountered in the solvated α polymer phase and the most stable domains of β phase.[15]

Extrusion

Orientation

The thermograms of the extrudates are illustrated in Figure 4. They show a slight drift of the baseline until 145°C [Fig. 4(a,c)]. A peak onset at 152°C is observed with a small shoulder peak at 156°C, followed by a sharp peak at 158°C and recovery at 170°C. No additional peaks are seen. From 152 to 170°C, an endothermic event of 34.7 J/g was calculated for the extrudate processed with slow cooling [Fig. 4(a)]. Comparison of this significant endothermic absorption with those observed in Figure 2(a) and 3(a), where the curves were completely flat and with slight absorption endotherm, respectively, leads us to propose three possible hypotheses:

1. appearance of a new product formed by chemical reaction (polymerization or break-

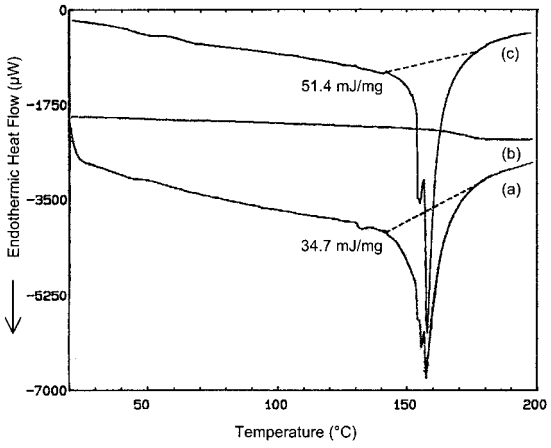

Figure 4 Influence of the cooling step in the hot-melt extrusion technique on the resulted material endotherm. DSC first run for (a) slowly and (c) fastly cooled extrudate; (b) DSC second run.

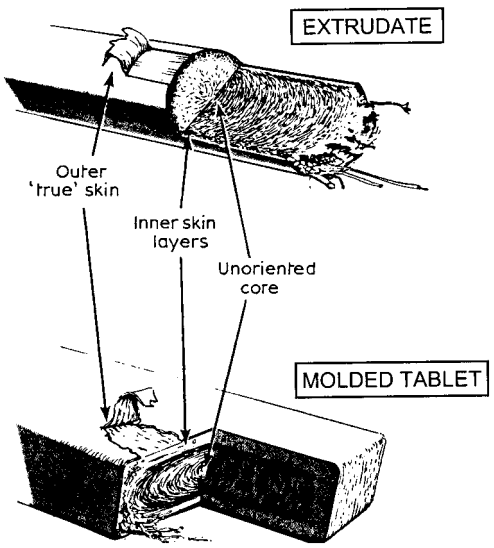

Figure 5 Difference in molecular structure according to the two processing techniques used, i.e., extrusion and compression molding.

down) during extrusion, due to high shear and temperature[17,18];
2. appearance of a crystalline structure[19];
3. appearance of an organized noncrystalline structure.[20]

Assumption 1 was not retained because both extrudate thermograms, during the second run [Fig. 4(b)], show an horizontal baseline with an absence of peaks. Assumption 2 was discarded because the thermogram of the milled extruded product is similar to that of Figure 2(a), where all the peaks between 130 and 180°C have disappeared. The particle size of the milled sample being approximately 60 μm, any expected crystalline structure will exhibit an unchanged thermogram compared to that before milling. Such behavior was not observed, and therefore no crystalline structure can be considered. This was also confirmed by X-ray and electron microscopic techniques.[21] It turns out that pullulan extrudates possess most probably some arranged or oriented structure. In fact, during extrusion, a gradient of shearing is established from the contact interface with the inside cylinder of the extruder towards the center. The shearing gradient[22,23] is maximum at the periphery and gradually decreases towards the center (Fig. 5). Consequently, a gradient of uniaxial polymer orientations takes place in the extrudate. Thus, a close connection appears between extrudate structure and thermogram profile. The drift of the base line between 20 and 147°C [Fig. 4(a)] is probably due to a layer of extrudate near the core and corresponds to a slightly oriented population of macromolecules. Above 147°C, it is especially the peripheral layer of the extrudate that is concerned, and the endothermic event corresponds to two largely oriented populations of polymers that appear at 152 and 156°C.

Thermodynamics of Microphase Formation

In the extrudate structure, the lowest chemical potential $(\mu_m)_\beta$ corresponds to segments involved in rigid polymer domains.[24,25] These domains, just like semicrystalline polymers, are characterized by a fluidization constant A_m related to the $(\mu_m)_\beta$ value,

$$\mu_m(l) - (\mu_m)_\beta = A_m RT \tag{4}$$

where $\mu_m(l)$ represents the chemical potential of the polymer segment in the liquid pure state.[24,25] Owing to the gradient of polymer uniaxial orientations, several A_m values exist and their corresponding $(\mu_m)_\beta$ values are much lower in the extrudate than in a simple physical blend. Hence, in opposition to the simple blend, the chemical potentials of solvated segments $(\mu_m)_\alpha$ in an extrudate could reach the value of the lowest $(\mu_m)_\beta$ values in different domains[15]:

$$\text{lowest } (\mu_m)_\alpha = \text{lowest } (\mu_m)_\beta \tag{5}$$

If the condition of the above equation is fulfilled, phase separation occurs and microphases are formed.[16] For each of these, eq. (5) may be written[26,27] as:

$$A_m + \frac{\ln \phi_p}{r} - \left(\frac{\bar{V}_m}{\bar{V}_S} - \frac{1}{r}\right)\phi_S + \chi_m \phi_S^2 = 0 \tag{6}$$

where $\bar{V}_m$ and $\bar{V}_S$ are the partial molar volumes of a polymer segment and the solvent respectively, ϕ_p and ϕ_S the volume fraction of the polymer and solvent respectively, r the number of segments per polymer and χ_m the Florry–Huggins interaction parameter. Equation (6) shows that during the extrusion process, phase separation is induced by orientation which is related to A_m term. High shear stress in the extruder capillary generates very sharp polymer orientations and large A_m values, which are responsible in eq. (6) for low

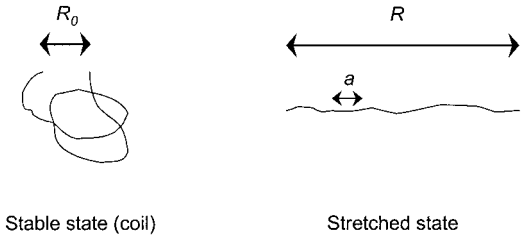

Figure 6 Polymer in stretched and stable state.

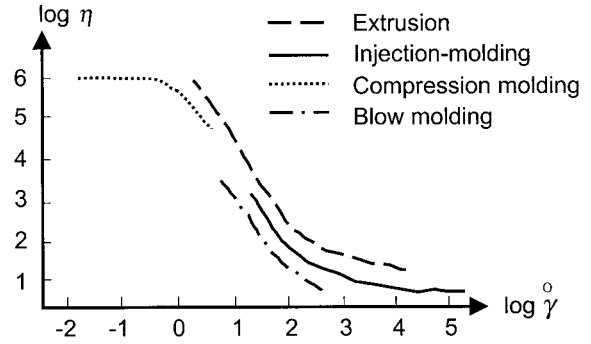

Figure 7 Shear ranges applied to polymers according to processes.

ϕ_p values and hence for microphase formation.[21] Phase separation occurs despite the favourable swelling conditions obtained at high temperature.

Cooling Treatment

Cooling of the extrudates at the die exit significantly changes the endotherm between 152 and 170°C, which increases from 34.7 to 51.4 J/g [Fig. 4(a,c)]. Endotherm values are closely related to the degree of orientation of the macromolecules in the extrudate. For a polymer chain, the structure thermodynamic equilibrium is reached when the distance R_0 between the two ends of the chain follows:

$$R_0^2 = ra^2 \tag{7}$$

where R_0 represents the end-to-end distance at coiling state, a the length of the elementary segment, and r the number of segments. In the die, stretching of macromolecules[28] increases R_0 to reach R (the end-to-end distance in the stretched state), but an elastic force of entropy f opposed to the stretching forces tends to decrease it:

$$f = 3kT\,\frac{R}{R_0^2} \tag{8}$$

From eq. (8), one can see that heating enhances the elastic force f, and as a result macromolecules in the stretched state move toward a coiled state (Fig. 6).

In contrast, a fast cooling decreases f and the interactions between streched macromolecules solidify the microstructure in its oriented state. It results that most of the macromolecules are kept oriented after extrusion, which explains the large increase of enthalpy of 16.7 J/g observed from Figure 4(a,c).

Compression Molding

Different processing parameters defining compression, compression molding, extrusion, and injection molding are listed in Table I. For compression molding, the applied shear rates are small[23,29] compared to extrusion (Fig. 7). Then, the probability that molecules create interactions (entanglements), which depend on the processing temperature and pressure, increases. These entanglements result from physical interactions and Brownian motion of molecule segments.

The thermogram obtained for a fastly cooled molded tablet [Fig. 8(a)] exhibits an endotherm of 11.9 J/g. By comparison to extrudate thermograms, the endotherm is narrower and less pronounced. When cooling occurs at a sufficiently

Table I Parameters Defining Different Processing Techniques

	Compression	Compression Molding	Melt Extrusion	Injection Molding
Applicable shear rate range ($\dot{\gamma}$)	—	10^{-1}–10^{1}s^{-1}	1–10^4 s^{-1}	10–10^5 s^{-1}
Applicable extensional rate magnitude ($\dot{\varepsilon}$)	—	+	+++	++
Processing parameters	P	P, T, $\dot{\gamma}$	P, T, $\dot{\gamma}$, $\dot{\varepsilon}$	P, T, $\dot{\gamma}$, $\dot{\varepsilon}$

[a] P: pressure; T: temperature; +: Low; ++: Medium; +++: High.

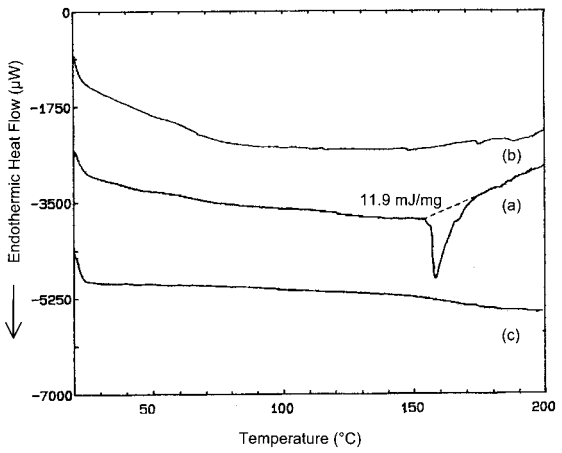

Figure 8 Influence of the cooling step in the compression molding technique on the resulted material endotherm. DSC first run for (a) fastly and (b) slowly cooled molded tablet; (c) DSC second run.

high rate, an abrupt contraction occurs and, because of the pressure, intermolecular distances are drastically decreased. A solidification process results in the immobilization of the structure due to increasing viscosity. The spatially homogeneous material does not present any long-range lattice order. The resulted structure is characterised by a lower A_m value compared to that obtained in the extrudates.

In contrast, the thermogram obtained for a slowly cooled molded tablet [Fig. 8(b)] exhibits a drift of the baseline. When cooling occurs at a sufficiently low rate, swelled polymer segments are formed and are involved in rigid polymer domains. The swelled, slowly cooled material exhibits quite different oriented structures and no phase separation, hence a drift shape endotherm is observed.

Study of Kinetic Disorientation

To investigate the isothermal transformation[30,31] of pullulan extrudates to the amorphous state, three different temperatures were chosen—namely 120, 125, and 130°C. After keeping the extrudate under these selected temperatures for 30 min, a DSC scan was run from 20 to 200°C at a rate of 12°C/min (Fig. 9).

The single endotherm observed in Figure 4(c) is split, after the thermal treatment, into a bimodal profile, which gives two distinct endotherms in Figure 9(c). The first and second peaks appear at 170 and 180°C, respectively. The latter appears in the same position as that for a physical mixture [Fig. 3(a)] when heating is performed at 12°C/min. This suggests that the second endotherm is related to the swelling reaction observed for the polymer–plasticizer blend [Fig. 3(a)], despite the fact that the extrudates were heated during the manufacturing process. Such a behavior is due to the microphase separation or formation of microphase structure. On the other hand, the first isotherm is due to the disorientation process of the different uniaxially oriented polymer populations. To summarize, Figure 9 shows the two mechanisms of swelling and disorientation hidden in the single endotherm of Figure 4(c).

To study the disorientation process, we can concentrate on the first disorientation endotherm ΔH_{disor}. It represents the enthalpy needed to disorient the remaining oriented macromolecule populations, that results from the thermal conditioning. If we now assume a first-order kinetic reaction for the disorientation process, we may write by analogy with the Arrhenius equation:

$$\ln\left[\frac{(\Delta H_{\text{destr}} - \Delta H_{\text{swell}})_f}{(\Delta H_{\text{destr}} - \Delta H_{\text{swell}})_i}\right] = \ln\left[\frac{(\Delta H_{\text{disor}})_f}{(\Delta H_{\text{disor}})_i}\right] = A \cdot \Delta t \cdot e^{-E_a/RT} \quad (9)$$

$$t_{1/2} = \frac{\ln 2}{k} = \frac{\ln 2}{Ae^{-E_a/RT}} \quad (10)$$

where ΔH_{swell} and ΔH_{destr} represent the enthalpies of swelling and destructuration (global processes), respectively. Subscripts i and f stand for the respective initial and final states that corre-

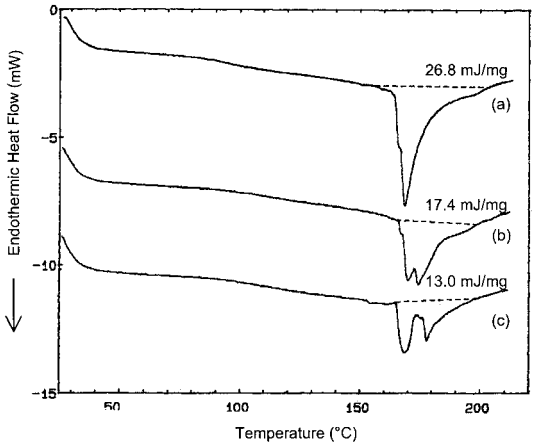

Figure 9 Thermograms recorded at 12°C/min scan rate after isothermal storage for 30 min at 120°C (a), 125°C (b), and 130°C (c).

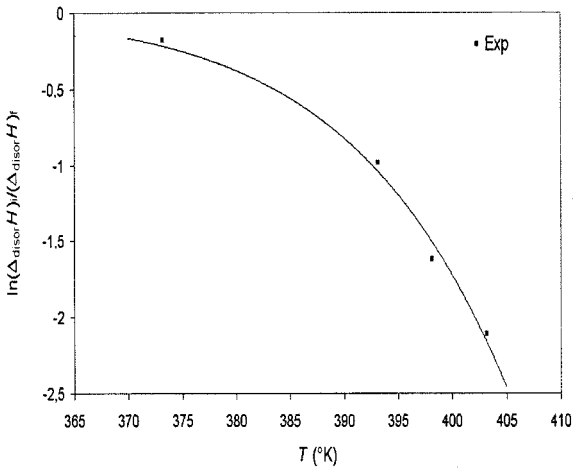

Figure 10 Relation between storage temperature and proportion of remaining oriented macromolecules structures.

spond to those before and after thermal treatment, E_a is the activation energy and $t_{1/2}$ is the half life. E_a and A are first obtained by exponential regression using eq. (9), then k, the rate constant, and $t_{1/2}$ are calculated from eq. (10). The calculated value of E_a is 1.38 J/g. Experimental results show a good correlation coefficient ($r^2 = 0.995$) for the regression over the range 100–130°C (Fig. 10), which is in agreement with the assumed first-order kinetics. The $t_{1/2}$ increases from 6 min at 125°C to 42 min at 100°C. Values cannot be extrapolated at lower temperatures. In fact, experiments performed on extrudates conditioned at 25°C during a period of 3 months give a reproductible endotherm of 51.4 J/g, which is related to the stable structure obtained at this temperature.

CONCLUSION

Processing parameters of both melt techniques have a great influence on the physicochemical properties of thermoplastic materials. Material characteristics were analyzed by DSC. Extrudates present gradient of uniaxial macromolecule orientations as well as microphase formation. The disorientation kinetics suggest two interpretative mechanisms connected to the extrudate microstructure. Fast cooling at the die exit enhances remained molecular orientation in the processed unit. In contrast, the compression molding process generates fairly oriented swelled structures due to the relatively low shear rate, especially when the molded tablet is slowly cooled. An unswelled structure results from an abrupt change in viscosity when the molded tablet is rapidly cooled. A kinetic study performed on the extrudates shows the stability of the structure at 25°C and the disorientation process at selected temperatures above 100°C. Finally, a knowledge of the processed material microstructure (i.e., orientation and microphase formation) can provide a useful basis for understanding and predicting drug release kinetics from solid dosage forms.

The authors are grateful to Dr. W. M. MacInnes, Nestlé Research Center, Lausanne, Switzerland, and Dr. E. G. Sarraf, Physical Institute of Condensed Matter, University of Lausanne, Switzerland, for helpful discussions.

REFERENCES

1. Nadella, H. P.; Henson, H. M.; Spruiell, J. E.; White, J. L. J Appl Polym Sci 1977, 21, 3003.
2. Choi, K. J.; Spruiell, J. E.; White, J. L. J Polym Sci 1982, 20, 27.
3. Kanai, T.; White, J. L. Polym Eng Sci 1984, 24, 1185.
4. Kanai, T.; Kimnna, M.; Schimizu, J. Sen-I Gakkaishi 1985, 14, T-139.
5. Plochoki, A. P.; Czarnecki, L. J Plastic Film Sheeting 1990, 6, 131.
6. Simpson, D. M.; Harrison, I. R. Antec 1991, 49, 203–205.
7. Follonier, N.; Doelker, E.; Cole, E. T. Drug Dev Ind Pharm 1994, 20, 1323.
8. Korsmeyer, R. W.; Peppas, N. A. In Controlled Release Delivery Systems; Roseman, T. J., Mansdorf, S. Z., Eds.; Marcel Dekker: New York, 1983; Chap 4.
9. Pavlov, G. M.; Korneeva, E. V.; Yevlampieva, N. P. Int J Biol Macromol 1994, 16, 318.
10. McIntyre, D. D.; Vogel, H. J. Starch 1993, 45, 406.
11. Young, A. H. U.S. Patent 3,312,559, 1967.
12. Stark, J. G.; Wallace, H. G. Chemistry Data Book; SI: London, 1976.
13. Khankari, R. K.; Law, D.; Grant, D. J. W. Int J Pharm 1992, 82, 117.
14. Spyriouni, T.; Economou, I. G.; Theodorou, D. N. Macromolecules 1997, 30, 4744.
15. Doi, M. Introduction to Polymer Physics; Clarendon Press: Oxford; 1996.
16. Olabisi, O. R.; Robeson, L. M.; Shaw, M. T. Polymer-Polymer Miscibility; Academic Press: New York, 1979.
17. El'darov, E. G.; Mamedov, F. V. Intern J Polymeric Mater 1995, 29, 1.
18. El'darov, E. G.; Mamedov, F. V.; Gol'dberg, V. M.; Zaikov, G. E. Oxidation Commun 1996, 19, 54.

19. Wunderlich, B. Macromolecular Physics; Academic Press: New York, 1980.
20. Bashir, Z.; Odell, J. A.; Keller, A. J Mat Sci 1986, 21, 3993.
21. Sarraf, A. G.; et al. To be published.
22. Harisson, P. J.; Newton, J. M.; Rowe, R. C. Int J Pharmaceutics 1987, 35, 235.
23. Schramm, G. A Practical Approach to Rheology and Rheometry; Haake Gmbh: Karlsruhe, Germany, 1994.
24. Small, P. A. J Appl Chem 1953, 3, 71.
25. Sarraf, E. G. J Chem Soc Faraday Trans 1997, 93, 2519.
26. Gardon, J. L. J Paint Technol 1966, 38, 43.
27. Huggins, M. L. J Phys Chem 1942, 46, 151.
28. Grosberg, A. Y.; Khokhlov, A. R. Ideal Polymer Chain; AIP Press: New York, 1994.
29. Addleman, R.; Barrie, T. Eur Plast News 1988, 15.
30. Gedde, U. W. Drug Dev Ind Pharm 1990, 16, 2465.
31. Flynn, J. H. J Thermal Anal 1991, 37, 293.